Understanding sources of atmospheric hydrogen chloride in coastal spring and continental winter

Andrea A. Angelucci[†], *Teles C. Furlani*[†], *Xuan Wang*[⁖], *Daniel J. Jacob*[‡⁂], *Trevor C. VandenBoer*[†], *Cora J. Young*[†]

†Department of Chemistry, York University, Toronto, Ontario, Canada M3J 1P3

⁖School of Energy and Environment, City University of Hong Kong, Kowloon, Hong Kong SAR, China

‡School of Engineering and Applied Sciences, Harvard University, Cambridge, Massachusetts, USA 02134

⁂Department of Earth and Planetary Sciences, Harvard University, Cambridge, Massachusetts, USA 02138

Ambient 0.5 Hz hydrogen chloride (HCl) measurements were made in Canadian cities to investigate chlorine activation and constrain the tropospheric chlorine budget. Springtime HCl mixing ratios in a coastal city (St. John's, NL) were up to 1200 parts per trillion by volume (pptv) with median of 63 pptv and were consistently elevated during daytime. High-time resolution measurements allowed attribution of events to general sources, including direct emissions. Most coastal HCl was related to sea salt aerosol acid displacement (R1) and chlorine activation. Continental urban (Toronto, ON) wintertime HCl mixing ratios reached up to 541 and 172 pptv, with medians of 67 and 11 pptv during two sampling periods characterized by different wind directions. The absence of consistent relationships with NOx, temperature, and wind direction, as well as a lack of diurnal patterns, suggested uncharacterized direct sources of HCl. One period with road salting occurred during sampling, but no relationship to changes in HCl observations was found. The contribution of road salt to the measured HCl may have been masked by larger contributors (such as direct sources of HCl) or perhaps the relationship between HCl and road salt application is not immediate and thus additional measurements over multiple salting events or between seasons would be required. GEOS-Chem modelled HCl temporal variations in mixing ratio agreed well with coastal measurements only. Measured mixing ratios were underestimated by the model in both locations, but to a greater degree (up to 3 orders of magnitude) in the continental city. The discrepancy between the model and measurements for the continental wintertime city emphasizes the need for greater understanding of direct sources of HCl and the impact of road salt.

Keywords: hydrogen chloride, reactive chlorine, cavity ring-down spectroscopy, GEOS-Chem, emissions, marine, continental, wintertime, road salt

Introduction

Reactive gas-phase chlorine (Cl^*) are species that can readily produce the chlorine atom ($ClNO_2$, HOCl, Cl_2, Cl_2O_2, $ClONO_2$, ClO, ClOO, OClO, BrCl, ICl). Atmospheric Cl* has been shown to impact the production of tropospheric ozone (O_3),[1] which negatively affects both human lung function and vegetation.[2,3] Ozone is produced photochemically through the oxidation of volatile organic compounds (VOCs) by hydroxyl radical (OH) and catalyzed by nitrogen oxides (NO_x = NO + NO_2). Chlorine atoms react similarly to OH in this cycle, but can produce more ozone per mole.[4] The chemical mechanisms responsible for this are not yet fully understood. The chlorine atom is also up to several times more reactive towards certain VOCs, relative to OH, and so can have a disproportionate impact towards the atmospheric budget of certain species-for example CH_4.[5]

Total gas-phase inorganic chlorine (Cl_y) includes all Cl^* species and hydrogen chloride (HCl). HCl acts as a major atmospheric reservoir of chlorine[6] and makes up the bulk of tropospheric Cl_y.[7] It is directly emitted from coal combustion[8], industrial sources (e.g. mining),[9] and biomass burning.[10] Formation of HCl also occurs through chemical reactions, two of which are thought to dominate in the troposphere.[11,12] The first is acid-displacement in which condensed phase soluble chloride (e.g. NaCl) reacts with another atmospheric acid (e.g. nitric acid, HNO_3) with HCl released into the gas phase (R1). The second is chlorine atom hydrogen abstraction (R2) from an organic molecule (RH). Chlorine atoms can be regenerated from heterogeneous chemistry that follows HCl partitioning back to aerosols. It can also be generated by the reaction of HCl with OH (R3), although this reaction is of minor importance in the troposphere.[13]

$$\mathbf{NaCl_{(aq)} + HNO_{3(g)} \rightleftharpoons HCl_{(g)} + NaNO_{3(aq)}} \quad \textbf{(R1)}$$

$$\mathbf{RH + Cl\bullet \rightarrow HCl + R\bullet} \quad \textbf{(R2)}$$

63 **$HCl + {\bullet}OH \rightarrow Cl{\bullet} + H_2O$** **(R3)**

64 HCl is predominantly removed from the troposphere through dry and wet deposition[6], which are
65 both major sinks for Cl_y. HCl has also been shown to potentially enhance haze and fog formation
66 in Delhi, India via gas-particle partitioning with aqueous aerosol, resulting in non-refractory
67 particulate chloride.[14] Given its importance in the makeup and fate of Cl_y, high quality
68 measurements of HCl are essential to constraining the chlorine budget.

69 Most HCl measurements have been previously made using carbonate-coated annular
70 denuders (e.g. [15]) or mist-chambers (e.g. [16]), which provide measurements on timescales of hours
71 to days. The low time-resolution limits insight into rapid sources and sinks of Cl_y. Recent
72 development of higher time-resolution techniques for measuring tropospheric HCl include
73 chemical ionization mass spectrometry (CIMS) and online ion chromatography (IC).[17,18,19]
74 Although these instruments are relatively widespread in the community, accurate calibration for
75 HCl is challenging. As a result, there have been few published high time resolution tropospheric
76 measurements of HCl including: ship measurements,[20,21] aircraft measurements over coastal and
77 continental environments,[6,7] as well as coastal and continental near-surface measurements.[22,23] The
78 majority of these measurements have been made in sea-spray impacted atmospheres, where the
79 acid-displacement mechanism of HCl production has been shown to dominate (R1). In general,
80 measurements of HCl range between ~10-700 parts-per-trillion-by-volume (pptv) across these
81 various environments.[7,20,22–25] Cavity ring-down spectroscopy (CRDS) is an emerging method for
82 measuring in-situ HCl that has been shown to be accurate and reliable, with high sensitivity.[22,24,26]

83 A few atmospheric models have included comprehensive Cl_y chemistry.[6,27,28] A recent
84 model developed by Wang *et al.* presents a simulation of tropospheric chlorine made with GEOS-
85 Chem.[6] It has explicit inclusion of chlorine mobilization from sea salt by acid-displacement of

HCl, as well as other heterogeneous processes. The GEOS-Chem model-predicted HCl compares well to surface and aircraft measurements in marine and rural-remote continental environments. Models have not been as extensively tested against surface HCl measurements in continental regions.[29]

In this work, we use a CRDS to make ambient 0.5 Hz HCl measurements in polluted coastal (St. John's, Newfoundland and Labrador) and continental (Toronto, Ontario) locations in Canada. These are high-time resolution surface measurements of HCl with high sensitivity and precision. We compare our observations to other measurements and model estimates of HCl made for locations expected to have similar chemistry, then use our measurements to assess chemistry and sources of Cl_y. Finally, we compare our measurements to the most recent representation of Cl_y chemistry in the GEOS-Chem model.

Methods

Measurement Locations and General Conditions

Atmospheric measurements were performed in two locations in Canada (Figure S1): i) St. John's, Newfoundland and Labrador (47.5728°N, 52.7225°W, 42 m above sea level) and ii) the Air Quality Research Station at York University, Toronto, Ontario (43.7738°N, 79.5071°W, 220 m above sea level). The St. John's measurements were collected from April 4–17, 2017 in a polluted marine boundary layer (BL) environment during early spring. The Toronto measurements were performed over two periods: from February 23–28, 2018 (denoted Period A) and from March 9–15, 2018 (Period B). Both were polluted urban continental atmospheres during winter.

HCl Measurements

Measurements of HCl were performed with two different Picarro G2108 HCl CRDS Analyzers with a precision of ±0.2 %, with a measurement frequency of 0.5 Hz. The instrument and its application towards tropospheric measurements are described in detail in Furlani et al. [26] In Furlani *et al.* it is stated that the response time of this instrument with a similar inlet setup to an on-off modulation of >10 ppbv HCl was 2-6 minutes.[26] We anticipate the response times of the system used here to be better than the previously described laboratory system due to several sharp features lasting <1min that were observed throughout our sampling periods. In St. John's, the lowest observations from the end of five days of continuous rain were used as background. In Toronto, the background was determined by overflowing the CRDS inlet with zero air and recording the observed value after a stable reading was obtained (approximately 60 minutes).[20] These background levels were determined both before and after performing measurements. The average of the two was used as the background. The backgrounds for St. John's and Toronto were measured to be 25±7 and 25±1pptv, respectively. Measured HCl data was corrected by subtraction of the background values for each location. The systems have background-corrected 0.5 Hz and 1-hour detection limits (LOD=3σ) of 20 and 3 pptv for the St. John's system, and 4 and 3 pptv for the Toronto system, respectively. The CRDS utilizes a 3-mirror high finesse cavity and a distributed feedback laser centered at 5739.2625 cm^{-1} to select for the vibrational absorption band of $H^{35}Cl$ and $H^{37}Cl$. The three high-reflectivity mirrors allow the instrument to attain a high path length of ~20 km. Three in-line filters before the CRDS cavity were used to prevent bias from particulate matter (PM). The first filter was a 2 μm polytetrafluoroethylene (PTFE) filter contained in a perfluoroalkoxy alkane (PFA) filter holder located ~2 cm upstream of the CRDS. The second

and third filters are built-in high efficiency particulate air (HEPA) filters installed within the CRDS, before the optical cavity.

In St. John's, a diaphragm pump was used to pull a flow of 10 L/min through a 2.4 m long ¼ inch PFA inlet. The HCl was sub-sampled at 2 L/min through a ¼ inch PFA tee into a 10 cm inlet line of the CRDS, resulting in an inlet residence time of about 1 second. By sub-sampling at a 90-degree angle from the 10 L/min flow, the amount of PM that can accumulate on the filters upstream of the instrument is reduced, particularly the coarse mode. The end of the inlet was located 4' below a large rain shelter. The inlet for the Toronto campaign was composed of 6 m of ¼ inch PFA tubing with a flow rate of 2 L/min, resulting in a residence time of about 13 seconds. The end of the inlet was fitted with a PTFE total suspended particulate inlet and rain cap. The sampling line was located inside a temperature-controlled room set to ~24°C. A potential negative bias under high RH conditions (RH >50 %) caused by inlet losses has been characterized for HCl measurements made with this CRDS.[26] The average RH was 61±19 % and 85±15 %, in Toronto and St. John's, respectively, which could lead to a negative bias up to 15 %, such that our reported mixing ratios represent lower limits. For comparison of HCl with supporting measurements or model output, the 0.5 Hz data was averaged onto the timescale of the lowest-frequency measurement.

Supporting Measurements

Supporting measurements for the St. John's observations included solar irradiance, NO and NO_2 ($\equiv NO_x$), O_3, and meteorological conditions. Meteorological data was obtained from the St. John's International Airport weather station (Table S1), approximately 5 km N of the sampling

site (47.62° N, 52.75° W). Solar irradiance was obtained from a regional weather station (47.38°N, 53.12°W) ~40 km W of the inlet location, due to the failure of a local irradiance sensor. Measurements of NO_x and O_3 were acquired from the National Air Pollution Surveillance (NAPS) Station (47.56° N, 52.71° W), ~2 km SE of the sampling site.

Additional measurements in Toronto were co-located with the HCl measurement, with chemical measurements sharing the same inlet. An American EcoTech EC9841 measured NO and NO_2 by chemiluminescence (Warren, RI; LOD = 400 pptv), an American EcoTech Serinus 10 measured O_3 by UV absorption spectrophotometry (LOD = 500 pptv), and a HOBO S-LIB-M003 Solar Radiation Smart Sensor measured irradiance (paired with a HOBO H21-USB Micro Station data logger). Measurements of O_3 and NO_x were obtained at 5-minute resolution, while solar irradiance was recorded every minute. Molybdenum converters found in chemiluminescence instruments can lead to interferences from some NO_z species (e.g. HONO and HNO_3) as they can also be converted to NO along with the desired NO_2. Even though the NO_2 measurement from this technique is technically NO_z+NO_2, we will refer to it as "NO_2" throughout since NO_2 mixing ratios are typically much greater than NO_z in the polluted urban environment of Toronto. Complimentary meteorology measurements were obtained from the York University ESSE Meteorological Observation Station (~0 m NW of the sampling site, Table S1). Air quality data (NO, NO_2, O_3, and $PM_{2.5}$) was obtained from government monitoring stations across Toronto, which include Toronto North (~4 km NE of sampling site), Toronto East (~20 km SE of sampling site), Toronto Downtown (~16 SE of sampling site), and Toronto West (~8 km SW of sampling site) stations (Figure S2).

GEOS-Chem Simulations

Simulations of HCl levels were done in GEOS-Chem version 11-02d (http://www.geos-chem.org) corresponding to the sampling times and locations described above. The model includes a detailed representation of ozone–NO_x–VOC–particulate matter–halogen chemistry, with an updated comprehensive treatment of chlorine chemistry.[6] The model is driven by GEOS-FP (Goddard Earth Observing System – Forward Processing) assimilated meteorological fields from the NASA Global Modeling and Assimilation office (GMAO) with native horizontal resolution of 0.25°×0.3125° and 72 vertical levels from the surface to the mesosphere. The simulation was conducted at that resolution over North America (60°–130°W, 10°–60°N), with dynamical boundary conditions from a global simulation with 4°×5° resolution. For the St. John's site (42 m above sea level), the model surface layer is presented for comparison with observation, which represents ≈998-1013 hPa (≈0-123 m above sea level). For the Toronto site (220 m above sea level), the second layer of model is presented for comparison, which represents about 983-998 hPa (≈123-254 m above sea level). The simulation included only natural sources for inorganic chlorine species. Supplementary data (i.e. NO and O_3) was also simulated for the Toronto observation periods. All modeled results are presented as hourly mean values.

Results and Discussions

HCl Observations

Coastal HCl mixing ratios (Table 1, Figure 1) ranged from < 20-1210 pptv (median of 63 pptv), with higher levels of HCl generally observed in the daytime. Previous measurements of HCl in coastal environments made with online IC and time-of-flight chemical ionization mass spectrometers (TOF-CIMS) have shown similar ranges with maximum levels of HCl between 140-4500 pptv.[19,30–33] We observed numerous (7) events of short-lived elevated HCl (on the order of

one to several hours), most of which (6) occurred during daytime. Five of these daytime events (April 9, 10, 11, 14 and 16) and the one nighttime event (night of April 6/7) showed fast HCl mixing ratio increases, >90 pptv/hr. Short-term temporal trends will be discussed in the next section.

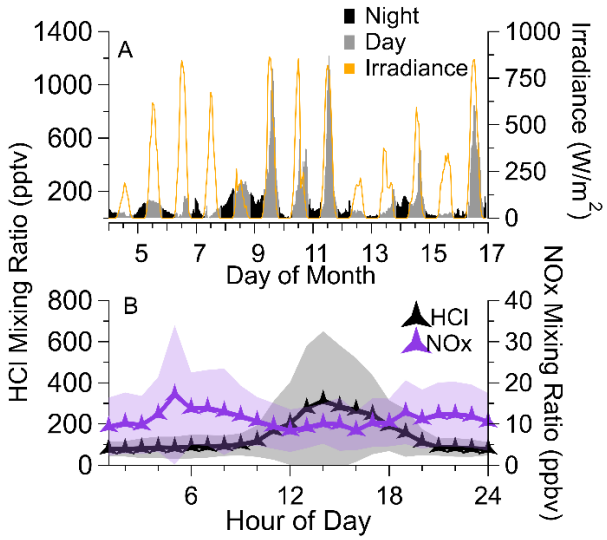

Figure 1: (A) Daytime (grey) and nighttime (black) HCl mixing ratios at 0.5 Hz, and solar irradiance (orange) from a coastal region (St. John's) in April 2017. Daytime here was defined as 7-18 h, representative of the average sunrise and sunset times for this observation period. (B) Diurnal plot of HCl and NOx in St. John's. The solid lines represent hourly means of HCl (black) and NOx (purple), respectively. The grey and purple shaded areas represent one standard deviation (σ, pptv) for the measured HCl and NOx, respectively.

The continental HCl measurements (Table 1, Figure 2) yielded a range of < 4-541 pptv for Period A and < 4-172 pptv for Period B, with medians of 67 and 11 pptv, respectively. Previous continental HCl measurements have been made with low-time resolution techniques such as denuders which have yielded high variability. Fewer high time-resolution measurements have been made inland but these have seen similar ranges.[34,35] Recently, HCl measurements were presented by McNamara *et al.* in wintertime Michigan using ambient ion monitor - ion chromatograph (AIM-

IC), with time resolution of 1 hour.[36] Their upper range of HCl was similar to that of Toronto (~240 pptv) with average levels between non-plume and plume periods being 126 ± 6 ppt and 103 ± 6 ppt, respectively. However, most of the data presented was below their LOD of 90 pptv. In the continental measurements, we observed three events (March 10, 11 and 12) in which HCl mixing ratios increased by >60 pptv/hr, each lasting about 1 hour. These will be discussed in detail below.

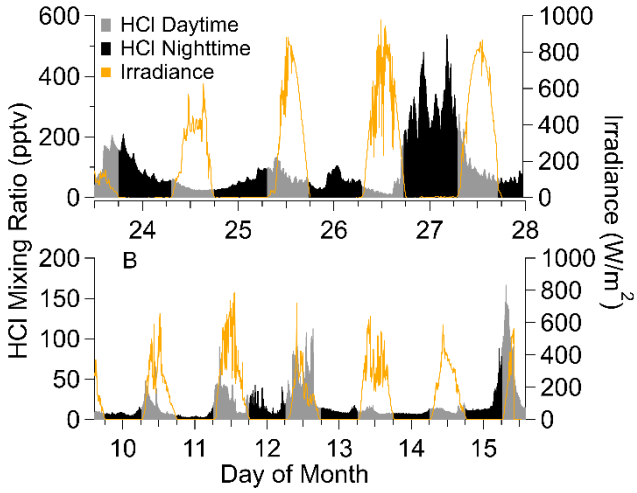

Figure 2: Daytime (grey) and nighttime (black) HCl mixing ratios collected at 0.5 Hz and solar irradiance (orange) from Toronto Period A in February (A) and Period B in March (B) 2018. Daytime here was defined as 7-18 h, representative of the average sunrise and sunset times for this observation period.

Comprehensive speciated Cl_y measurements were made over the coastal ocean and continental northeastern United States during the WINTER aircraft campaign, in February and March 2015. These measurements made with the same instrument in both coastal and continental locations provide a useful comparison for our observations. Median HCl mixing ratios over land during WINTER were 113 pptv (nighttime) and 100 pptv (daytime), while those over ocean were 305 pptv (nighttime) and 329 pptv (daytime).[7] Our continental HCl measurements are comparable to the over land mixing ratios. Our coastal measurements are lower than their mixing ratios

measured over the ocean. This may be a result of the lower population density around St. John's compared to the northeastern United States, which leads to lower NOx levels,[37] and subsequently lower levels of the Cl_y precursors HNO_3 and N_2O_5. Differences in seasonality may also drive differences between our measured data and those of others in the continental setting as WINTER occurred during February-March while the measurements in St. John's occurred in April. Seasonal variation in available OH (i.e. lower OH levels in winter) can drive seasonal variability in HNO_3 production downwind of NO_x sources.[38] Consistent with the measurements described above, our coastal HCl observations are higher than our continental observations (Table 1).

Table 1: Maximum, minimum, and median (overall, day, and night) mixing ratios of HCl measured by CRDS and modelled by GEOS-Chem for coastal St. John's and continental Toronto sampling periods.

Location	Dates	Type	Rate	HCl (pptv) Maximum	Minimum	Median	Median Day	Median Night
St John's	April 4-17, 2017	Measured	0.5 Hz	1210	<20	63	96	45
		Measured	1 hr	1119	21	62	94	46
		Modelled	1 hr	255	7.49	24.0	28.1	24.0
Toronto (Period A)	February 23-28, 2018	Measured	0.5 Hz	541	<4	67	58	67
		Measured	1 hr	446	12	65	59	71
		Modelled	1 hr	11.5	<1	<1	<1	<1
Toronto (Period B)	March 9-16, 2018	Measured	0.5 Hz	172	<4	11	15	9
		Measured	1 hr	137	<4	11	14	9
		Modelled	1 hr	3.95	<1	<1	<1	<1

Coastal Measurements

In our coastal measurements there are multiday and hours-timescale features in the observed HCl mixing ratios. The multiday features correspond to long and broad HCl cycles lasting 1-2 days. We observed four of these cycles during our measurements. These cycles exhibited continued HCl production lasting ~23 hours before reaching their maximum in daytime

(Figure S3). The multiday features increased at an average rate of 10 ± 4 pptv/hr before reaching their maxima. Coastal environments have abundant chloride from both marine aerosol and interface surfaces (e.g. ground and buildings) that can form HCl by reacting with HNO_3 through acid-displacement (R2).[6] Maximum HCl during these periods (313 pptv) was reached in the mid-afternoon (Figure 1B), which is generally consistent with the photochemical production and accumulation of HNO_3 from measurements made in similar coastal locations.[39,40] Although we do not have measurements of HNO_3, production is well-established to follow a reproducible diurnal trend, typically maximizing shortly after solar noon.[34,41,42] However, the sustained HCl during nighttime cannot be explained by R2, suggesting another, as-yet-unidentified mechanism may be contributing. The fast features (hours-timescale) had a higher rate of change in HCl compared to the multiday ones. Most of the former were observed to maximize during daytime and one at night. The single nighttime event was observed on the night of April 6/7, in which HCl levels rapidly increased by ~50 pptv/hr (Figure S5). Based on news reports and wind direction, the observed nighttime HCl is suspected to originate from an urban fire that occurred < 700 m from the sampling location that destroyed a large building, releasing HCl from the combustion of its materials.

The highest HCl levels were observed during the daytime during three of these several-hour cycles. During these events, mixing ratios increased at a rate of 165 ± 27 pptv/hr (n=3), reaching a maximum of 1060 ± 157 pptv. These short-lived features were observed in the presence of increased solar irradiance that occurred near mid-day (Figures 3, S4). The temporal relationship between short-lived fast rates of change in HCl and available sunlight could be caused by several factors. Meteorological changes that would be expected with increased sunlight include decreased relative humidity and increased temperature and mixing. At elevated temperatures and low humidity, with atmospheric composition held constant, a shift in thermodynamic equilibrium can

occur. This could cause volatile particle chloride (e.g. NH_4Cl) to partition into gas-phase HCl. However, volatile chlorine-containing species are rarely observed in appreciable quantities under atmospherically relevant conditions.[43,44] We observed that changes in temperature and relative humidity are temporally offset from the increases in HCl (Figure 3). This suggests that partitioning is not the dominant source of the observed increase in HCl. At this location, average wind speeds observed prior to the rapid increases in HCl mixing ratios were 6.5 m/s, which is within the range of critical speeds (5-7 m/s) that ensure complete mixing in the BL.[45] Entrainment mixing could also be a source of HCl if levels are elevated aloft. Recent work showed that mixing ratios of HCl have little vertical variation in the troposphere.[46] In addition, measured HCl mixing ratios above the BL and below 30km altitude[6,23,47] are generally similar to those observed near the surface,[22,33,34] suggesting entrainment mixing is not a major source of HCl to the surface. In contrast, paired surface and aircraft observations in coastal atmospheres have demonstrated enhancements of $ClNO_2$ aloft,[48] which could serve as a source of Cl* to the surface.[7] Lastly, direct emission of HCl does not appear to be related to these events. According to the National Pollutant Release Inventory (NPRI), there are no industrial sources of HCl on the island of Newfoundland. Combustion processes also appear unimportant as levels of NO_x are relatively constant during daylight hours and not correlated with HCl (Figure 3). However, without direct tracers such as CO for combustion, this cannot be completely ruled out. We argue that the most likely explanation for the fast HCl events is photolysis of Cl* with increasing irradiance as the source of our observed daytime HCl. Photolabile Cl^* species such as $ClNO_2$ and Cl_2 are precursors to the chlorine atom and may form from heterogeneous reactions on sea-salt aerosols present in this NO_x-rich environment.[12,16]

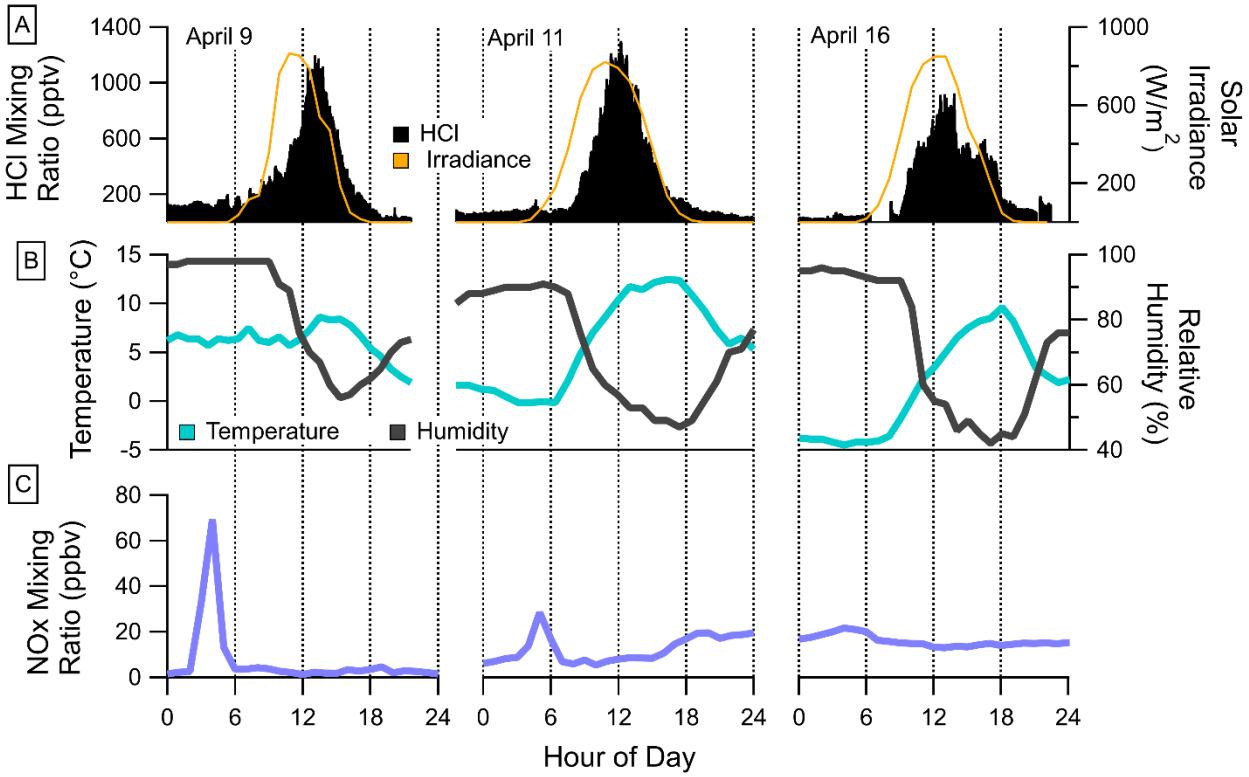

Figure 3: Measurements for April 9, 11, and 16, 2017 in which short-lived increases of HCl were observed in St. John's. (A) HCl mixing ratios (black) and solar irradiance (orange); (B) temperature (black) and relative humidity (turquoise); and (C) NO_x mixing ratios.

Levels of photolabile Cl* species that have been observed in the polluted marine BL and the residual layer are high enough to generate the observed levels of HCl, specifically the reports of $ClNO_2$ mixing ratios.[7] Those levels which have previously been observed are in the hundreds of pptv to greater than 3 ppbv range in coastal cities of North America and could be mixed to the surface from residual layer reservoirs formed at night.[4,7,49] Due to the short lifetime of the chlorine atom (e.g.[50]), HCl is expected to form rapidly via its reaction with organics (R3). Maximum HCl levels coincident with high solar irradiance occur around midday or early afternoon. For photolysis of photolabile Cl* to be the driving process, the reservoir would have to persist into midday (~6 hours after sunrise), rather than undergoing complete photolysis shortly after sunrise. In Pasadena, California (34.14 °N) during late spring, $ClNO_2$ present at sunrise was fully photolyzed by noon (~6 hours after sunrise) on sunny days.[48] Mielke *et al.* observed the persistence of $ClNO_2$ and Cl_2

into midday (~7 hours after sunrise) in Calgary, Alberta (51.08 °N) during early spring.[51] During April 2010 weather conditions in Calgary, which is ~3.5 °N of St. John's, were sunny during the daytime.[51] Weather conditions during our measurements in St. John's during April 2017 were a mix of cloud, snow, and rain. This suggests irradiance in St. John's was similar or lower than Calgary and that $ClNO_2$ and Cl_2 could persist well into the day. We observed that levels of HCl reached their maximum on three days in April near mid-day and coincident with maximum solar irradiance, consistent with a photolabile precursor photolysis source of HCl. Overall, we conclude that acid-displacement, direct emissions, and photolysis are active in this coastal environment. This dataset suggests that photolysis of photolabile precursors contribute to HCl accumulation before noon and may also dominate HCl production on some days with elevated irradiance. Our high-time resolution measurements allow us to better distinguish between these mechanisms and understand their relative importance to the chlorine budget.

Continental Measurements

No repeatable temporal variations in HCl mixing ratio were observed in our continental measurements. However, intermittent elevated mixing ratios of HCl were seen on February 23, 26, and 27 (Period A), as well as March 12 and 15 (Period B), which occurred during both daytime and nighttime. Elevated HCl levels that occurred during the morning do not have a reproducible relationship with the typical diurnal pattern of traffic-related NO_x, suggesting that combustion of fuel by the transportation sector is not an important source of our measured HCl (Figures 4, S6, S7). There is no clear evidence of the HCl temporal patterns that would be expected from acid displacement (R1, i.e. local maximum midday to late afternoon) or Cl atom reaction (R2, i.e. local maximum early to midday). High levels of NO were always present at our sampling site (confirmed through comparison to the Toronto North Air Quality Station (Figure S2)), which would preclude

local N_2O_5 chemistry and subsequent formation of photolabile precursors, such as $ClNO_2$. This may not be the case upwind of the observation site where N_2O_5 formation and ensuing chemistry with aerosol chloride could form HCl prior to the airmass intersecting the NO source. Regardless, the morning increases in HCl that start around 4 am occur too early in the day to be attributed to photolysis of labile Cl-atom precursors and is likely from primary emission sources of HCl and chemical processing of Cl^--containing aerosols (e.g. water treatment plants, electrical power generators, refineries, waste disposal, and incinerators).[20,52] We now consider each of these cases in more detail.

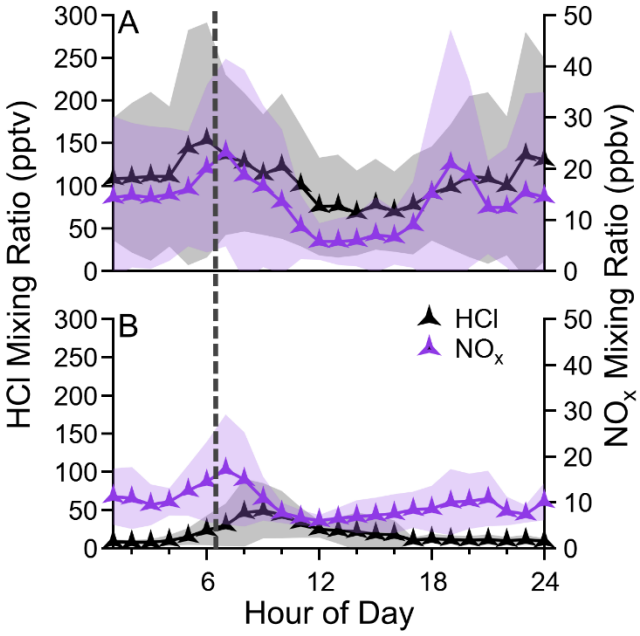

Figure 4: Diurnal plots of HCl and NOx for our Toronto dataset for Period A (A) and Period B (B). Period A was February 23–28, 2018 (denoted Period A) and Period B was March 9–15, 2018 The solid lines represent hourly means of HCl (black) and NOx (purple), respectively. The grey and purple shaded areas represent one standard deviation (σ, pptv) for HCl and NOx, respectively. The grey dashed line represents the average sunrise time (~06:30).

Wind data for Period A (Figure S6) showed predominantly southwesterly winds, while Period B showed predominantly northwesterly winds. These two wind regimes were verified using

the Hybrid Single-Particle Lagrangian Integrated Trajectory (HYSPLIT) model back trajectories (Figure S7).[53–56] The background levels of HCl always present at the sampling site for Period A (74 ± 4 pptv) were significantly higher (t-test: $p<0.001$) than Period B (11 ± 1 pptv, Figure 4, Table S2**).** Difference in wind direction between the two periods (Figure S6) may indicate different sources of regional pollution in the atmospheric fetch of the observation site. This is consistent with observed trends of other pollutants in the Toronto area (e.g. O_3[57]). Southwest of our sampling location are several potential sources of HCl, according to the NPRI, that may have contributed to background levels of pollution including a waste management plant (≈32 km SSW), a soap manufacturing facility (≈20 km SSW), as well as iron and steel mills (≈63 km SSW). These sources are reported to have emitted 0.07, 0.171, and 1.4 tonnes of HCl, respectively, in 2017.[58] The same database shows that no major HCl pollution sources exist within ≈ 100 km northwest of our inlet. This supports the assertion of regional pollution sources in the different air masses during Periods A and B altering the observed background HCl mixing ratios.

We observed several cases of elevated nocturnal levels of HCl and NO_x coinciding with lower windspeeds and low temperatures. Although we do not have a direct measurement of BL height this suggests that higher HCl is present during low BL height events. This occurred in particular during Period B in which lower temperatures were observed (Figure S10). In Period A, we observed elevated levels of NO between 14-52 ppbv, concurrent with rapid increases of HCl at night with sharp transitions, especially on the night of February 27 (Figure S11). These observations of high NO_x mixing ratios were verified via comparison to the nearest government air quality station (Toronto North, Figure S2). This suggests some transport of local emissions of combustion-related HCl during Period A. The regional source of HCl was also located within the nocturnal BL or we would not observe these elevated levels as the BL height decreased. The HCl

event on the night of February 27 was not the only instance in which an abrupt decrease in wind speed accompanied an increase in HCl. This type of event was prevalent throughout our sampling period both during day and night. The ability to capture these sudden changes in HCl highlight the utility of these high-time resolution measurements in capturing point, local, and regional sources.

A potential precursor of Cl_y that is not well understood is road salt, which can act as a source of chloride directly, but also through road spray aerosol suspension and subsequent deposition on other urban surfaces (e.g. as a component of grime).[59] Urban centers and watersheds, in particular, have been shown to be chronically saturated with chloride from road salt application.[60,61] Aerosolization has been estimated to remove 20-40% of the total salt from roads, which in turn increases sodium and chloride $PM_{2.5}$ levels in the winter.[41,62] Road salt has recently been identified as the primary source of aerosol chloride in an urban wintertime environment, accounting for 80-100% of $ClNO_2$ formation.[36] Road salt could also theoretically contribute to HCl formation through acid displacement (R1), though this has not been quantified using ambient measurements. During our Toronto sampling, there was one major snow event on March 12 and a few isolated snow flurries (March 13 and 14) in which road salt and/or salt brine was applied to ground surfaces.[6364,65] The day of the snow event as well as the last day of Period B showed sustained production of HCl starting in the early morning (Figure S12). The timing of the increase suggests that fresh road salt may have temporarily facilitated formation of HCl through (R1) or (R2). Meteorological conditions for these days can be seen in Figure S13. The most recent major salting events prior to Periods A and B occurred 7 days before the start of sampling, on February 16 and March 2, respectively. Mass concentrations of $PM_{2.5}$ chloride were obtained at three-day intervals (Figure S12) from two NAPS stations within 10 km of our sampling site. Average mass concentrations of $PM_{2.5}$ chloride across both stations were 0.04 ± 0.01 and 0.17 ± 0.11 $\mu g/m^3$, for

periods A and B, respectively. These are consistent with known salt applications during the two sampling periods and previous $PM_{2.5}$ chloride measurements made in a similar wintertime continental urban environment.[62] These suggest that road salt likely plays a role in Cl_y chemistry in continental urban regions. However, because of the limited number of confirmed road salt applications during our measurement period, we cannot directly relate observed HCl to these applications. This emphasizes the need for improved understanding of the role of road salt as a source of HCl in wintertime urban environments.

Model Comparison

To determine the magnitude of the discrepancy between the observations and known HCl sources, a comparison with the recently updated GEOS-Chem chlorine scheme was made. The GEOS-Chem model was able to reproduce the general background of HCl mixing ratios as well as the temporal variations on certain days in the coastal environment but underestimated mixing ratios by a factor of 2-5 (Table 1, Figure S15); while for the continental region, the model was unable to reproduce variations in HCl mixing ratios and underestimated mixing ratios by 1-3 orders of magnitude (Figures S16 and S17). Our measured HCl ranges are significantly greater than those predicted in the simulation (t-test: $p < 0.001$ all locations, nearly all periods, Table S3). Diurnal variations in HCl were predicted by the model for both locations, which we observed in coastal St. John's but not continental Toronto (Figures S15-S17). The model does not include direct sources of anthropogenic HCl from the available emission inventory for our measurement locations because they were created in the 1990s and have been shown to be inaccurate.[20,27] A TOMCAT simulation that included an emission inventory for HCl can be compared to our measurements.[27] That model is within a factor of 2 for St. John's and 35 for Toronto, but always high (Figure S16). As described above, our simulations which exclude direct emissions, are always lower than our

421 measurements; being within a factor of 2-5 for St. John's and 1-3 orders of magnitude for Toronto.
422 The same GEOS-Chem simulation we used recently was able to accurately reproduce chlorine
423 chemistry for China when a detailed chlorine emission inventory was included.[29] From this we
424 conclude that direct emissions of HCl are crucial to constraining the chlorine budget, particularly
425 in continental areas. In addition, current schemes do not include road salt as a source of chloride
426 because information on source strength is lacking, despite the chemistry likely following that of
427 sea salt. Road salt is a major reservoir of chlorine in wintertime continental regions and there is
428 increasing evidence in the literature of its importance to the Cl_y budget.[36,62] Direct sources of HCl
429 need to be identified and quantified, along with identifying the role of road salt and its chemical
430 processing, so that continental chlorine chemistry can be more accurately represented in models.

431 The model is generally more capable at predicting HCl levels measured in coastal areas in
432 comparison to our urban continental observations in Toronto. The role of direct sources is less
433 important in coastal environments as expected, and the aerosol chloride reservoir is simulated
434 accurately.[6] This supports our observations that the HCl levels in St. John's seemed to be largely
435 affected by acid-displacement and photolabile precursors derived from marine chloride. Since
436 these Cl-reservoirs and their associated chemical mechanisms are more complete in the model, the
437 GEOS-Chem simulation for that location is more accurate. As described above, the observations
438 are consistent with a contribution from photolysis of photolabile Cl* in the production of HCl in
439 coastal St. John's. The ability of GEOS-Chem to credibly simulate $ClNO_2$ chemistry well may be
440 another reason as to why this location has better agreement with the simulations.[6] The
441 underestimate of measured coastal HCl is likely because the small city of St. John's is the major
442 source of anthropogenic pollution in the model grid-box in which it is located, which could lead

to a representativeness error (i.e. sampling error of the observation grid) between our ground measurements and the spatially averaged model output.

Conclusion & Atmospheric Implications

Ambient measurements of HCl were made using high time-resolution (0.5 Hz) cavity ring-down spectroscopy (CRDS) in a springtime coastal (St. John's, NL) and wintertime continental (Toronto, ON) region in order to better understand chlorine activation and constrain the chlorine budget in the troposphere. Mixing ratios of HCl were up to 1200 and 541 pptv, respectively, in the coastal and continental regions. Coastal measurements showed evidence for HCl production via photolysis of photolabile precursors, resulting in rapid increases in HCl, as well as through acid displacement. Continental HCl mixing ratios did not exhibit these features and instead seemed to be more influenced by direct emission sources of HCl from local to regional scales. Although a road salting event occurred during the sampling period it showed no obvious relation to measured HCl, which may be due to a masking effect caused by more significant regional sources. Our observations in both regions were compared to GEOS-Chem simulations. The modeled temporal variations in HCl for the coastal region agreed well with our measurements on certain days but modeled mixing ratios for the continental region underestimated measurements by up to 3 orders of magnitude. These findings highlight the limitations of models in simulating a continental wintertime city, indicating that a better understanding of direct HCl emissions as well as the potential effects of road salt applications is needed.

Associated Content

Maps, figures, and tables as described in the text.

Author Information

Corresponding Author

E-mail: youngcj@yorku.ca

Present Address

Department of Chemistry, York University, Toronto, Ontario, Canada

Notes

The authors declare no competing financial interest.

Acknowledgements

Funding was provided by the Natural Sciences and Engineering Research Council. We thank Kathryn Dawe for assistance with the St. John's HCl measurements, Bob Redmond for providing St. John's supporting data, and Stephen Miller and Peter Taylor for Toronto meteorology data. We acknowledge the Environmental Canada National Air Pollution Surveillance Network and Analysis and Air Quality Section as well as the Ontario Ministry of the Environment, Conservation and Parks Section for supporting measurements including NO_x, O_3, and $PM_{2.5}$.

References

(1) Tanaka, P. L.; Riemer, D. D.; Chang, S.; Yarwood, G.; McDonald-Buller, E. C.; Apel, E. C.; Orlando, J. J.; Silva, P. J.; Jimenez, J. L.; Canagaratna, M. R.; Neece, J. D.; Mullins, C. B.; Allen, D. T. Direct Evidence for Chlorine-Enhanced Urban Ozone Formation in Houston, Texas. *Atmos Environ* **2003**, *37*, 1393–1400.

(2) Lippmann, M. Health Effects of Tropospheric Ozone: Review of Recent Research Findings and Their Implications to Ambient Air Quality Standards. *J Expo Anal Environ*

Epidemiol **1993**, *3* (1), 103—129.

(3) Ainsworth, E. A.; Yendrek, C. R.; Sitch, S.; Collins, W. J.; Emberson, L. D. The Effects of Tropospheric Ozone on Net Primary Productivity and Implications for Climate Change. *Annu Rev Plant Biol* **2012**, *63* (1), 637–661. https://doi.org/10.1146/annurev-arplant-042110-103829.

(4) Osthoff, H. D.; Roberts, J. M.; Ravishankara, A. R.; Williams, E. J.; Lerner, B. M.; Sommariva, R.; Bates, T. S.; Coffman, D.; Quinn, P. K.; Dibb, J. E.; Stark, H.; Burkholder, J. B.; Talukdar, R. K.; Meagher, J.; Fehsenfeld, F. C.; Brown, S. S. High Levels of Nitryl Chloride in the Polluted Subtropical Marine Boundary Layer. *Nat Geosci* **2008**, *1* (5), 324–328.

(5) Platt, U.; Allan, W.; Lowe, D. Hemispheric Average Cl Atom Concentration from $^{13}C/^{12}C$ Ratios in Atmospheric Methane. *Atmos Chem Phys* **2004**, *4* (9/10), 2393–2399. https://doi.org/10.5194/acp-4-2393-2004.

(6) Wang, X.; Jacob, D. J.; Eastham, S. D.; Sulprizio, M. P.; Zhu, L.; Chen, Q.; Alexander, B.; Sherwen, T.; Evans, M. J.; Lee, B. H.; Haskins, J. D.; Lopez-Hilfiker, F. D.; Thornton, J. A.; Huey, G. L.; Liao, H. The Role of Chlorine in Global Tropospheric Chemistry. *Atmos Chem Phys* **2019**, *19* (6), 3981–4003. https://doi.org/10.5194/acp-19-3981-2019.

(7) Haskins, J. D.; Jaeglé, L.; Shah, V.; Lee, B. H.; Lopez-Hilfiker, F. D.; Campuzano-Jost, P.; Schroder, J. C.; Day, D. A.; Guo, H.; Sullivan, A. P.; Weber, R.; Dibb, J.; Campos, T.; Jimenez, J. L.; Brown, S. S.; Thornton, J. A. Wintertime Gas-Particle Partitioning and Speciation of Inorganic Chlorine in the Lower Troposphere over the Northeast United States and Coastal Ocean. *J Geophys Res Atmos* **2018**, *123* (22), 12,897-12,916. https://doi.org/10.1029/2018JD028786.

(8) Liu, Y.; Fan, Q.; Chen, X.; Zhao, J.; Ling, Z.; Hong, Y.; Li, W. Modeling the Impact of Chlorine Emissions from Coal Combustion and Prescribed Waste Incineration on Tropospheric Ozone Formation in China. *Atmos. Chem. Phys.* **2018**, *18*, 2709–2724. https://doi.org/10.5194/acp-18-2709-2018.

(9) Keene, W. C.; Khalil, M. A. K.; Erickson, D. J.; McCulloch, A.; Graedel, T. E.; Lobert, J.

M.; Aucott, M. L.; Gong, S. L.; Harper, D. B.; Kleiman, G.; Midgley, P.; Moore, R. M.; Seuzaret, C.; Sturges, W. T.; Benkovitz, C. M.; Koropalov, V.; Barrie, L. A.; Li, Y. F. Composite Global Emissions of Reactive Chlorine from Anthropogenic and Natural Sources: Reactive Chlorine Emissions Inventory. *J Geophys Res* **1999**, *104*, 8429–8440.

(10) Lobert, J. M.; Keene, W. C.; Logan, J. A.; Yevich, R. Global Chlorine Emissions from Biomass Burning: Reactive Chlorine Emissions Inventory. *J Geophys Res* **1999**, *104*, 8373–8389. https://doi.org/10.1029/1998JD100077.

(11) Leu, M.-T.; Timonen, R. S.; Keyser, L. F.; Yung, Y. L. Heterogeneous Reactions of HNO3(g) + NaCl(s)→ HCl(g) + NaNO3(s) and N2O5(g) + NaCl(s)→ ClNO2(g) + NaNO3(S). *J Phys Chem* **1995**, *03*, 13203–13212. https://doi.org/10.1021/j100035a026.

(12) Faxon, C. B.; Allen, D. T. Chlorine Chemistry in Urban Atmospheres: A Review. *Environ Chem* **2013**, *10* (3), 221–233. https://doi.org/10.1071/EN13026.

(13) Keene, W. C.; Stutz, J.; Pszenny, A. A. P.; Maben, J. R.; Fischer, E. V.; Smith, A. M.; von Glasow, R.; Pechtl, S.; Sive, B. C.; Varner, R. K. Inorganic Chlorine and Bromine in Coastal New England Air during Summer. *J Geophys Res Atmos* **2007**, *112* (10), 1–15. https://doi.org/10.1029/2006JD007689.

(14) Gunthe, S. S.; Liu, P.; Panda, U.; Raj, S. S.; Sharma, A.; Darbyshire, E.; Reyes-Villegas, E.; Allan, J.; Chen, Y.; Wang, X.; Song, S.; Pöhlker, M. L.; Shi, L.; Wang, Y.; Kommula, S. M.; Liu, T.; Ravikrishna, R.; McFiggans, G.; Mickley, L. J.; Martin, S. T.; Pöschl, U.; Andreae, M. O.; Coe, H. Enhanced Aerosol Particle Growth Sustained by High Continental Chlorine Emission in India. *Nat Geosci* **2021**. https://doi.org/10.1038/s41561-020-00677-x.

(15) United States Environmental Protection Agency. *Compendium of Methods for the Determination of Inorganic Compounds in Ambient Air: Determination of Reactive Acidic and Basic Gases and Strong Acidity of Atmospheric Fine Particles (<2.5 Mm) (Compendium Method IO-4.2)*; 1999.

(16) Maben, J. R.; Keene, W. C.; Pszenny, A. A. P.; Galloway, J. N. Volatile Inorganic Cl in Surface Air over Eastern North America. *Geophys Res Lett* **1995**, *22* (24), 3513–3516.

https://doi.org/10.1029/95GL03335.

(17) Markovic, M. Z.; VandenBoer, T. C.; Murphy, J. G. Characterization and Optimization of an Online System for the Simultaneous Measurement of Atmospheric Water-Soluble Constituents in the Gas and Particle Phases. *J Environ Monit* **2012**, *14* (7), 1872. https://doi.org/10.1039/c2em00004k.

(18) Roberts, J. M.; Veres, P.; Warneke, C.; Neuman, J. A.; Washenfelder, R. A.; Brown, S. S.; Baasandorj, M.; Burkholder, J. B.; Burling, I. R.; Johnson, T. J.; Yokelson, R. J.; de Gouw, J. Measurement of HONO, HNCO, and Other Inorganic Acids by Negative-Ion Proton-Transfer Chemical-Ionization Mass Spectrometry (NI-PT-CIMS): Application to Biomass Burning Emissions. *Atmos Meas Tech* **2010**, *3* (4), 981–990. https://doi.org/10.5194/amt-3-981-2010.

(19) Oms, M. T.; Jongejan, P. A. C.; Veltkamp, A. C.; Wyers, G. P.; Slanina, J. Continuous Monitoring of Atmospheric HCl, HNO2 , HNO3 and SO2 by Wet-Annular Denuder Air Sampling with On-Line Chromatographic Analysis. *Int J Environ Anal Chem* **1996**, *62* (3), 207–218. https://doi.org/10.1080/03067319608028134.

(20) Crisp, T. A.; Lerner, B. M.; Williams, E. J.; Quinn, P. K.; Bates, T. S.; Bertram, T. H. Observations of Gas Phase Hydrochloric Acid in the Polluted Marine Boundary Layer. *Journal of Geophysical Research*. 2014, pp 6897–6915. https://doi.org/10.1002/2013JD020992.

(21) Vollmer, M. K.; Mühle, J.; Henne, S.; Young, D.; Rigby, M.; Mitrevski, B.; Park, S.; Lunder, C. R.; Rhee, T. S.; Harth, C. M.; Hill, M.; Langenfelds, R. L.; Guillevic, M.; Schlauri, P. M.; Hermansen, O.; Arduini, J.; Wang, R. H. J.; Salameh, P. K.; Maione, M.; Krummel, P. B.; Reimann, S.; O'Doherty, S.; Simmonds, P. G.; Fraser, P. J.; Prinn, R. G.; Weiss, R. F.; Paul Steele, L. Unexpected Nascent Atmospheric Emissions of Three Ozone-Depleting Hydrochlorofluorocarbons. *Proc Natl Acad Sci U S A* **2021**, *118* (5). https://doi.org/10.1073/pnas.2010914118.

(22) Hagen, C. L.; Lee, B. C.; Franka, I. S.; Rath, J. L.; Vandenboer, T. C.; Roberts, J. M.; Brown, S. S.; Yalin, A. P. Cavity Ring-down Spectroscopy Sensor for Detection of Hydrogen Chloride. *Atmos Meas Tech* **2014**, *7* (2), 345–357. https://doi.org/10.5194/amt-

7-345-2014.

(23) Wang, X.; Jacob, D. J.; Downs, W.; Zhai, S.; Zhu, L.; Shah, V.; Christopher, D.; Alexander, B.; Evans, M. J.; Eastham, S. D.; Andrew, J.; Veres, P.; Koenig, T. K.; Volkamer, R.; Huey, L. G.; Thomas, J.; Percival, C. J.; Lee, B. H.; Thornton, J. A. Global Tropospheric Halogen (Cl , Br , I) Chemistry and Its Impact on Oxidants. *Atmos. Chem. Phys. Discuss.* **2021**, No. June, 1–34.

(24) Dawe, K. E. R.; Furlani, T. C.; Kowal, S. F.; Kahan, T. F.; Vandenboer, T. C.; Young, C. J. Formation and Emission of Hydrogen Chloride in Indoor Air. *Indoor Air* **2019**, *29*, 70–78. https://doi.org/10.1111/ina.12509.

(25) Jeong, D.; Seco, R.; Gu, D.; Lee, Y.; Nault, B. A.; Knote, C. J.; Mcgee, T.; Sullivan, J. T.; Jimenez, J. L.; Campuzano-jost, P.; Blake, D. R.; Sanchez, D.; Guenther, A. B.; Tanner, D.; Huey, L. G.; Long, R.; Anderson, E.; Hall, S. R.; Ullmann, K.; Shin, H.; Herndon, S. C.; Lee, Y.; Kim, D.; Ahn, J.; Kim, S. Integration of Airborne and Ground Observations of Nitryl Chloride in the Seoul Metropolitan Area and the Implications on Regional Oxidation Capacity During KORUS-AQ 2016. *Atmos. Chem. Phys.* **2019**, *19* (19), 12779--12795. https://doi.org/10.5194/acp-19-12779-2019.

(26) Furlani, T. C.; Veres, P. R.; Dawe, K. E.; Neuman, J. A.; Brown, S. S.; VandenBoer, T. C.; Young, C. J. Validation of a New Cavity Ring-down Spectrometer for Measuring Tropospheric Gaseous Hydrogen Chloride. Accepted. *Atmos Meas Tech*. https://doi.org/https://doi.org/10.5194/amt-2021-105.

(27) Hossaini, R.; Chipperfield, M. P.; Saiz-Lopez, A.; Fernandez, R.; Monks, S.; Feng, W.; Brauer, P.; Von Glasow, R. A Global Model of Tropospheric Chlorine Chemistry: Organic versus Inorganic Sources and Impact on Methane Oxidation. *J Geophys Res* **2016**, *121* (23), 14,271-14,297. https://doi.org/10.1002/2016JD025756.

(28) Thornton, J. A.; Kercher, J. P.; Riedel, T. P.; Wagner, N. L.; Cozic, J.; Holloway, J. S.; Dube, W. P.; Wolfe, G. M.; Quinn, P. K.; Middlebrook, A. M.; Alexander, B.; Brown, S. S. A Large Atomic Chlorine Source Inferred from Mid-Continental Reactive Nitrogen Chemistry. *Nature* **2010**, *464* (11), 271–274. https://doi.org/10.1038/nature08905.

(29) Wang, X.; Jacob, D. J.; Fu, X.; Wang, T.; Le, M.; Hallquist, M.; Liu, Z.; Mcduffie, E.; Liao, H. Effects of Anthropogenic Chlorine on PM2.5 and Ozone Air Quality in China. *Environ Sci Technol* **2020**, *In press*. https://doi.org/10.1021/acs.est.0c02296.

(30) Keene, W. C.; Pszenny, A. A. P.; Maben, J. R.; Stevenson, E.; Wall, A. Closure Evaluation of Size-Resolved Aerosol PH in the New England Coastal Atmosphere during Summer. *J Geophys Res D Atmos* **2004**, *109* (23), 1–16. https://doi.org/10.1029/2004JD004801.

(31) Marcy, T. P.; Gao, R. S.; Northway, M. J.; Popp, P. J.; Stark, H.; Fahey, D. W. Using Chemical Ionization Mass Spectrometry for Detection of HNO3, HCl, and ClONO2in the Atmosphere. *Int J Mass Spectrom* **2005**, *243* (1), 63–70. https://doi.org/10.1016/j.ijms.2004.11.012.

(32) Kim, S.; Huey, L. G.; Stickel, R. E.; Pierce, R. B.; Chen, G.; Avery, M. A.; Dibb, J. E.; Diskin, G. S.; Sachse, G. W.; McNaughton, C. S.; Clarke, A. D.; Anderson, B. E.; Blake, D. R. Airborne Measurements of HCl from the Marine Boundary Layer to the Lower Stratosphere over the North Pacific Ocean during INTEX-B. *Atmos. Chem. Phys. Discuss.* **2008**, *8*, 3563–3595.

(33) Bari, A.; Ferraro, V.; Wilson, L. R.; Luttinger, D.; Husain, L. Measurements of Gaseous HONO, HNO3, SO2, HCl, NH3, Particulate Sulfate and PM2.5 in New York, NY. *Atmos Environ* **2003**, *37* (20), 2825–2835. https://doi.org/10.1016/S1352-2310(03)00199-7.

(34) Dasgupta, P. K.; Campbell, S. W.; Al-Horr, R. S.; Ullah, S. M. R.; Li, J.; Amalfitano, C.; Poor, N. D. Conversion of Sea Salt Aerosol to NaNO3 and the Production of HCl: Analysis of Temporal Behavior of Aerosol Chloride/Nitrate and Gaseous HCl/HNO3 Concentrations with AIM. *Atmos Environ* **2007**, *41* (20), 4242–4257. https://doi.org/10.1016/j.atmosenv.2006.09.054.

(35) Appel, B. R.; Tokiwa, Y.; Povard, V.; Kothny, E. L. The Measurement of Atmospheric Hydrochloric Acid in Southern California. *Atmos Environ Part A, Gen Top* **1991**, *25* (2), 525–527. https://doi.org/10.1016/0960-1686(91)90325-2.

(36) McNamara, S. M.; Kolesar, K. R.; Wang, S.; Kirpes, R. M.; May, N. W.; Gunsch, M. J.;

Cook, R. D.; Fuentes, J. D.; Hornbrook, R. S.; Apel, E. C.; China, S.; Laskin, A.; Pratt, K. A. Observation of Road Salt Aerosol Driving Inland Wintertime Atmospheric Chlorine Chemistry. *ACS Cent Sci* **2020**, *6* (5), 884–694. https://doi.org/10.1021/acscentsci.9b00994.

(37) Oliver, J. G. J.; Bouwmana, A. F.; Van der Hoek, K. W.; Berdowski, J. J. M. Global Air Emission Inventories for Anthropogenic Sources of NOx, NH3 and N2O in 1990. *Environ Pollut* **1998**, *102*, 135–148. https://doi.org/10.1016/S0269-7491(98)80026-2.

(38) Wang, G.; Jia, S.; Li, R.; Ma, S.; Chen, X.; Wu, Z.; Shi, G.; Niu, X. Seasonal Variation Characteristics of Hydroxyl Radical Pollution and Its Potential Formation Mechanism during the Daytime in Lanzhou. *J Environ Sci (China)* **2020**, *95*, 58–64. https://doi.org/10.1016/j.jes.2020.03.045.

(39) Dibb, J. E.; Scheuer, E.; Whitlow, S. I.; Vozella, M.; Williams, E.; Lerner, B. M. Ship-Based Nitric Acid Measurements in the Gulf of Maine during New England Air Quality Study 2002. *J Geophys Res D Atmos* **2004**, *109* (20), 1–14. https://doi.org/10.1029/2004JD004843.

(40) Kanaya, Y.; Tanimoto, H.; Matsumoto, J.; Furutani, H.; Hashimoto, S.; Komazaki, Y.; Tanaka, S.; Yokouchi, Y.; Kato, S.; Kajii, Y.; Akimoto, H. Diurnal Variations in H2O2, O3, PAN, HNO3 and Aldehyde Concentrations and NO/NO2 Ratios at Rishiri Island, Japan: Potential Influence from Iodine Chemistry. *Sci Total Environ* **2007**, *376* (1–3), 185–197. https://doi.org/10.1016/j.scitotenv.2007.01.073.

(41) Patra, A.; Colvile, R.; Arnold, S.; Bowen, E.; Shallcross, D.; Martin, D.; Price, C.; Tate, J.; ApSimon, H.; Robins, A. On Street Observations of Particulate Matter Movement and Dispersion Due to Traffic on an Urban Road. *Atmos Environ* **2008**, *42* (17), 3911–3926. https://doi.org/10.1016/j.atmosenv.2006.10.070.

(42) Zheng, J.; Zhang, R.; Fortner, E. C.; Volkamer, R. M.; Molina, L.; Aiken, A. C.; Jimenez, J. L.; Gaeggeler, K.; Dommen, J.; Dusanter, S.; Stevens, P. S.; Tie, X. Measurements of HNO3 and N2O5 Using Ion Drift-Chemical Ionization Mass Spectrometry during the MILAGRO/MCMA-2006 Campaign. *Atmos Chem Phys* **2008**, *8* (22), 6823–6838. https://doi.org/10.5194/acp-8-6823-2008.

(43) Du, H.; Kong, L.; Cheng, T.; Chen, J.; Yang, X.; Zhang, R.; Han, Z.; Yan, Z.; Ma, Y. Insights into Ammonium Particle-to-Gas Conversion: Non-Sulfate Ammonium Coupling with Nitrate and Chloride. *Aerosol Air Qual Res* **2010**, *10* (6), 589–595. https://doi.org/10.4209/aaqr.2010.04.0034.

(44) Zhang, Q.; Jimenez, J. L.; Canagaratna, M. R.; Allan, J. D.; Coe, H.; Ulbrich, I.; Alfarra, M. R.; Takami, A.; Middlebrook, A. M.; Sun, Y. L.; Dzepina, K.; Dunlea, E.; Docherty, K.; DeCarlo, P. F.; Salcedo, D.; Onasch, T.; Jayne, J. T.; Miyoshi, T.; Shimono, A.; Hatakeyama, S.; Takegawa, N.; Kondo, Y.; Schneider, J.; Drewnick, F.; Borrmann, S.; Weimer, S.; Demerjian, K.; Williams, P.; Bower, K.; Bahreini, R.; Cottrell, L.; Griffin, R. J.; Rautiainen, J.; Sun, J. Y.; Zhang, Y. M.; Worsnop, D. Ubiquity and Dominance of Oxygenated Species in Organic Aerosols in Anthropogenically-Influenced Norther Hemisphere Midlatitudes. *Geophys Res Lett* **2007**, *34*, L13801, doi:10.1029/2007GL029979.

(45) Van De Wiel, B. J. H.; Moene, A. F.; Jonker, H. J. J.; Baas, P.; Basu, S.; Donda, J. M. M.; Sun, J.; Holtslag, A. A. M. The Minimum Wind Speed for Sustainable Turbulence in the Nocturnal Boundary Layer. *J Atmos Sci* **2012**, *69* (11), 3116–3127. https://doi.org/10.1175/JAS-D-12-0107.1.

(46) Nara, S.; Sato, T.; Yamada, T.; Fujinawa, T.; Kuribayashi, K.; Manabe, T.; Froidevaux, L.; Livesey, N.; Walker, K.; Xu, J.; Schreier, F.; Orsolini, Y.; Limpasuvan, V.; Kuno, N.; Kasai, Y. Validation of the Vertical Profiles of HCl over the Wide Range of the Stratosphere to the Lower Thermosphere Measured by SMILES. *Atmos Meas Tech Discuss* **2020**, 1–25. https://doi.org/10.5194/amt-2020-105.

(47) Wilkerson, J.; Sayres, D.; Smith, J.; Allen, N.; Rivero, M.; Greenberg, M.; Martin, T.; Anderson, J. In Situ Observations of Stratospheric HCl Using Three-Mirror Integrated Cavity Output Spectroscopy. *Atmos Meas Tech* **2021**, *14* (5), 3597–3613. https://doi.org/10.5194/amt-14-3597-2021.

(48) Young, C. J.; Washenfelder, R. A.; Roberts, J. M.; Mielke, L. H.; Osthoff, H. D.; Tsai, C.; Pikelnaya, O.; Stutz, J.; Veres, P. R.; Cochran, A. K.; Vandenboer, T. C.; Flynn, J.; Grossberg, N.; Haman, C. L.; Lefer, B.; Stark, H.; Graus, M.; De Gouw, J.; Gilman, J. B.;

Kuster, W. C.; Brown, S. S. Vertically Resolved Measurements of Nighttime Radical Reservoirs in Los Angeles and Their Contribution to the Urban Radical Budget. *Environ Sci Technol* **2012**, *46* (20). https://doi.org/10.1021/es302206a.

(49) Mielke, L. H.; Stutz, J.; Tsai, C.; Hurlock, S.; Roberts, J. M.; Veres, P. R.; Froyd, K.; Hayes, P.; Cubison, M.; Jimenez, J. L.; Washenfelder, R. A.; Young, C. J.; Gilman, J. B.; de Gouw, J.; Flynn, J.; Grossberg, N.; Lefer, B.; Liu, J.; Weber, R.; Osthoff, H. D. Heterogeneous Formation of Nitryl Chloride and Its Role as a Nocturnal NOx Reservoir Species during CalNex-LA 2010. *J Geophys Res* **2013**, *118*, 10638–10652. https://doi.org/10.1002/jgrd.50783.

(50) Young, C. J.; Washenfelder, R. A.; Edwards, P. M.; Parrish, D. D.; Gilman, J. B.; Kuster, W. C.; Mielke, L. H.; Osthoff, H. D.; Tsai, C.; Pikelnaya, O.; Stutz, J.; Veres, P. R.; Roberts, J. M.; Griffith, S.; Dusanter, S.; Stevens, P. S.; Flynn, J.; Grossberg, N.; Lefer, B.; Holloway, J. S.; Peischl, J.; Ryerson, T. B.; Atlas, E. L.; Blake, D. R.; Brown, S. S. Chlorine as a Primary Radical: Evaluation of Methods to Understand Its Role in Initiation of Oxidative Cycles. *Atmos Chem Phys* **2014**, *14*, 3427–3440.

(51) Mielke, L. H.; Furgeson, A.; Osthoff, H. D. Observation of ClNO 2 in a Mid-Continental Urban Environment. *Environ Sci Technol* **2011**, *45* (20), 8889–8896. https://doi.org/10.1021/es201955u.

(52) Riedel, T. P.; Bertram, T. H.; Crisp, T. A.; Williams, E. J.; Lerner, B. M.; Vlasenko, A.; Li, S.-M.; Gilman, J.; de Gouw, J.; Bon, D. M.; Wagner, N. L.; Brown, S. S.; Thornton, J. A. Nitryl Chloride and Molecular Chlorine in the Coastal Marine Boundary Layer. *Environ Sci Technol* **2012**, *46*, 10463–10470. https://doi.org/10.1021/es204632r.

(53) Draxler, R. R.; Hess, G. D. Description of the HYSPLIT_4 Modeling System. NOAA Tech. Memo. ERL ARL-224, NOAA Air Resources Laboratory, Silver Spring, MD, 24 Pp. **1997**, No. November 2010.

(54) Draxler, R. R. HYSPLIT4 User's Guide. NOAA Tech. Memo. ERL ARL-230, NOAA Air Resources Laboratory, Silver Spring, MD. 1999.

(55) Draxler, R. R.; Hess, G. D. An Overview of the HYSPLIT_4 Modelling System for

Trajectories, Dispersion and Deposition. *Aust Meteorol Mag* **1998**, *47* (4), 295–308.

(56) Stein, A. F.; Draxler, R. R.; Rolph, G. D.; Stunder, B. J. B.; Cohen, M. D.; Ngan, F. NOAA's HYSPLIT Atmospheric Transport and Dispersion Modeling System. *Bull Am Meteorol Soc* **2015**, *96* (12), 2059–2077. https://doi.org/10.1175/BAMS-D-14-00110.1.

(57) Geddes, J. A.; Murphy, J. G.; Wang, D. K. Long Term Changes in Nitrogen Oxides and Volatile Organic Compounds in Toronto and the Challenges Facing Local Ozone Control. *Atmos Environ* **2009**, *43* (21), 3407–3415. https://doi.org/10.1016/j.atmosenv.2009.03.053.

(58) Environment and Climate Change Canada: NPRI Data Search – Facility Search Results Hydrochloric acid, available at: https://pollution-waste.canada.ca/national-release-inventory/ archives/index.cfm,.

(59) Baergen, A. M.; Styler, S. A.; Van Pinxteren, D.; Müller, K.; Herrmann, H.; Donaldson, D. J. Chemistry of Urban Grime: Inorganic Ion Composition of Grime vs Particles in Leipzig, Germany. *Environ Sci Technol* **2015**, *49* (21), 12688–12696. https://doi.org/10.1021/acs.est.5b03054.

(60) Corsi, S. R.; De Cicco, L. A.; Lutz, M. A.; Hirsch, R. M. River Chloride Trends in Snow-Affected Urban Watersheds: Increasing Concentrations Outpace Urban Growth Rate and Are Common among All Seasons. *Sci Total Environ* **2015**, *508*, 488–497. https://doi.org/10.1016/j.scitotenv.2014.12.012.

(61) Oswald, C. J.; Giberson, G.; Nicholls, E.; Wellen, C.; Oni, S. Spatial Distribution and Extent of Urban Land Cover Control Watershed-Scale Chloride Retention. *Sci Total Environ* **2019**, *652*, 278–288. https://doi.org/10.1016/j.scitotenv.2018.10.242.

(62) Kolesar, K. R.; Mattson, C. N.; Peterson, P. K.; May, N. W.; Prendergast, R. K.; Pratt, K. A. Increases in Wintertime PM2.5 Sodium and Chloride Linked to Snowfall and Road Salt Application. *Atmos Environ* **2018**, *177* (November 2017), 195–202. https://doi.org/10.1016/j.atmosenv.2018.01.008.

(63) TO Winter Operations (@TO_WinterOps). Salt brine will be applied to hills and bridges this evening. Please keep a safe distance behind the trucks. Twitter, March 12, 2018.

https://twitter.com/TO_WinterOps/status/973203680647368705 (accessed Jun 30, 2020).

(64) TO Winter Operations (@TO_WinterOps). In response to isolated flurries, salt trucks were out where required last evening and overnight on expressways and main roads. The Humber Bay Waterfront Trail, Martin Goodman Trail and the separated bike lanes downtown were also salted. Twitter, March 13, 2018. https://twitter.com/TO_WinterOps/status/973513105878802433 (accessed Jun 30, 2020).

(65) TO Winter Operations (@TO_WinterOps). Salters are out across the city this morning in response to isolated flurries. Twitter, March 14, 2018. https://twitter.com/TO_WinterOps/status/973894963074301952 (accessed Jun 30, 2020).

TOC Art